Astron. Astrophys. 238, 50–58 (1990)

ASTRONOMY AND ASTROPHYSICS

Binary galaxies with dark halos

I. Dynamics

D.S.L. Soares*

Kapteyn Astronomical Institute, University of Groningen, Postbus 800, NL-9700 AV Groningen, The Netherlands

Received April 14, 1989; accepted March 28, 1990

Abstract. The dynamics of binary galaxies is considered using a two-component mass model for spiral galaxies. The mass model has a "visible", and an extended "dark" component. The gravitational potential of a binary system, consisting of two such galaxies, is calculated. The effect of overlapping mass distributions, in the potential calculation, is fully considered. Orbits of binary galaxies are also calculated.

Observational predictions are examined by means of simulation of a sample of binary galaxies. The simulation consists of a Monte Carlo generation of three-dimensional orbits, that are subsequently projected onto the plane of sky. A qualitative comparison with recent work by Schweizer is made.

The combined effect of overlapping mass distributions and merging on binary dynamics is a depletion of high velocity differences at small projected separations. The main conclusion is that there may be a considerable difference in derived orbit and intrinsic galaxy properties between the usual point-mass approximation and the more realistic model presented here.

Key words: galaxies: binary – galaxies: spiral – galaxies: structure of – galaxies: kinematics and dynamics of

1. Introduction

Here we develop and discuss a simple model for binary galaxies which incorporates as a main feature the presence of an extended dark mass component. The model has a simple analytical description that enables it to be used in a Monte Carlo algorithm for the distribution of orbital parameters of binaries. This is the first paper of a series, devoted to a statistical study of binaries, in which individual galaxies are represented by extended mass distributions. We begin by investigating the orbits.

The statistical approach to binary galaxy studies has been widely used since Holmberg's initial work (Holmberg, 1937; Page, 1952; Turner, 1976; Peterson, 1979; White, 1981; White et al., 1983; Karachentsev, 1985; van Moorsel, 1987; Schweizer, 1987; Oosterloo, 1988). However, all of this work relies upon a Keplerian treatment of binary orbits in which the galaxies are assumed to be point masses.

Rotation curve studies of individual spiral galaxies indicate the presence of dark halos (e.g., van Albada and Sancisi, 1986). It is worthwhile, then, to improve the treatment of orbits of binary galaxies using a model in which each galaxy in a pair has a dark component that is properly taken into account in the pair potential well.

In addition to the investigation of the force field in binary systems, in which the individual galaxies are surrounded by dark halos, we perform Monte Carlo simulations of binary galaxy orbits, and apply them to an analysis of the recent work by Schweizer (1987). Schweizer makes use of Monte Carlo simulations, with a point-mass model, in order to find the best fitting parameters to a well-defined sample of binaries. The results show that Schweizer's point-mass model fails to reproduce the predictions made with the more realistic approach adopted here, namely, the depletion of high velocity differences at the small separation range, and, that not only orbital eccentricity is important in the distribution of velocities and separations but also the shape of the mass distribution in the galaxies.

In Sect. 2 we introduce the model for the galaxy mass distribution. The mass distributions can overlap in the course of their motion in the mutual gravitational potential; the "overlapping" force field is calculated. Orbits are calculated in Sect. 3. Section 4 is dedicated to the simulations, and the main results are discussed in Sect. 5.

2. Truncated dark halo approximation

The two-component mass distribution used here is an attempt to reproduce the main characteristic of spiral galaxies, that is to say, the presence of an extended dark mass component in addition to the stellar mass. The galaxy is rigid, in the sense that the overall mass distribution does not suffer any kind of deformation during orbital motion in a binary system. The dark component is truncated at a given outer radius, beyond which the force is $\propto 1/r^2$. Below, we describe the model in some detail.

2.1. Model galaxy

The density distribution of the "visible" component is represented by a Plummer sphere (polytrope of index 5):

$$\rho_G(R)=\frac{3M}{4\pi}\frac{R_c^2}{(R^2+R_c^2)^{5/2}}, \tag{1}$$

yielding the cumulative mass distribution:

$$M_G(R)=\frac{MR^3}{(R^2+R_c^2)^{3/2}}, \tag{2}$$

* Present address: Observatório Astronomico da Piedade, Depto. de Física, ICEx, UFMG, C.P. 702, 30161 Belo Horizonte, MG, Brazil

where M is the total mass of visible matter, and R_c is the core radius of the visible component.

The gravitational potential of the distribution given by Eq. 1 is

$$\Psi_G(R)=\frac{-GM}{(R^2+R_c^2)^{1/2}}. \tag{3}$$

One does not need to truncate the Plummer sphere. This distribution extends to infinity but it is highly centrally concentrated: 94% of the total mass is contained within $R_G=5\times R_c$, which we identify with the de Vaucouleurs' radius of the galaxy (R_{25}).

For the purposes we have in mind, i.e., a study of the orbital motions of galaxies in a binary system, it is not necessary to go into more detail concerning the model of the visible galaxy, such as, the consideration of a more realistic disk-like mass distribution. What we wish to reproduce is the general trend of the visible mass profile, that is, a central mass concentration, and a declining density as one moves to the outer regions of the visible body. The choice of a more sophisticated mass model to represent the visible component is only important when considering pair interactions on galactic scales, as it happens to occur in a close encounter (Barnes, 1988; Borne, 1988, and references therein). In a statistical study of binary galaxies, the fine features obtained with such a detailed modelling are irrelevant, because we are interested in the distribution of binary properties on all scales, but not particularly on galactic ones. On the contrary, those are to be excluded because they belong to the domain of merging processes. In such a domain we cannot speak anymore about a binary system as a well-defined entity. Furthermore, the evaluation of the visible mass using the circular velocity at a given radius is at most 25% higher if one assumes spherical symmetry instead of a more realistic disk-like mass distribution (van Moorsel, 1982b). This factor can be fully included in the statistical analysis.

The dark component is modeled by an approximate isothermal sphere, with a core (Kent, 1987). The density distribution is given by:

$$\rho_H(R)=\frac{\sigma^2}{2\pi G(R^2+a^2)}, \quad R\le R_H, \tag{4a}$$

$$\rho_H(R)=0, \quad R>R_H, \tag{4b}$$

where σ is the velocity dispersion in the halo, and a its core radius. This distribution leads to a flat rotation curve, at large radii, with an asymptotic rotational velocity of $\sqrt{2}\sigma$.

The halo is truncated at some outer radius, R_H, which is a free parameter of the model defining the distribution of dark matter.

We can now write the expression for the mass as a function of radius in the halo:

$$M_H(R)=\frac{2\sigma^2 a}{G}\left(\frac{R}{a}-\arctan\frac{R}{a}\right), \quad R\le R_H, \tag{5a}$$

$$M_H(R)=\frac{2\sigma^2 a}{G}\left(\frac{R_H}{a}-\arctan\frac{R_H}{a}\right), \quad R>R_H. \tag{5b}$$

The gravitational potential produced by the truncated halo is given by:

$$\Psi_H(R)=\frac{-2\sigma^2 a}{R}\left[\frac{R}{a}-\arctan\frac{R}{a}+\frac{R}{2}\ln\left(\frac{R_H^2+a^2}{R^2+a^2}\right)\right], \quad R\le R_H, \tag{6a}$$

$$\Psi_H(R)=\frac{-2\sigma^2 a}{R}\left(\frac{R_H}{a}-\arctan\frac{R_H}{a}\right), \quad R>R_H. \tag{6b}$$

In Fig. 1 we show a plot of the rotation curve of the halo-galaxy (HG) model. The dashed lines represent the rotation curves of the two separate mass components.

The model galaxy, with its two components, has five parameters: M, R_c, σ, a, and R_H. They must be chosen in such a way that the resulting rotation curve is approximately flat. For the purpose of this paper only the combined potential is important. Thus, without loss of generality, we can choose the contribution of the disk such that it dominates in the inner region. In analysis of rotation curves this is called the *maximum-disk approximation*; the flatness of the rotation curve is then attributed to the *disk-halo conspiracy* (see, e.g., van Albada and Sancisi, 1986). This approach reduces the number of truely free parameters of the mass model to two: the velocity of the flat part of the rotation curve, V_c, and the cut-off radius of the halo, R_H. Because, observationally, the shape of the rotation curve in the inner region is closely related to V_c (Rubin et al., 1985), the two disk parameters M and R_c are fixed by the choice of V_c. In turn, V_c and R_c determine the halo parameters σ and a.

The galaxy shown in Fig. 1, represented by its rotation curve, has $M=1.0$, $R_c=0.2$, $\sigma=2.1$, $a=0.6$, and $R_H=4.0$. The implied dark mass is 6.2 units. The mass unit is $10^{11}\ M_\odot$, the length unit is 10 kpc, and the time unit is 10^8 yr. In these units $G=4.497$, and velocities are given in units of 97.8 km s^{-1}.

The model is used below for an investigation of the radial force field in a binary system consisting of two equal galaxies. The mass distributions of the galaxies overlap as their centers get closer than $2\times R_H$.

2.2. *Calculation of the overlapping potential*

Given the galaxy model, the next step towards orbits of binary galaxies is the calculation of the mutual gravitational potential of two such galaxies. When $r\ge R_{H1}+R_{H2}$ the binary potential is the usual Keplerian one. For $r<R_{H1}+R_{H2}$, the Poisson equation must be solved, by means of a numerical integration, inside the two overlapping spherical mass distributions.

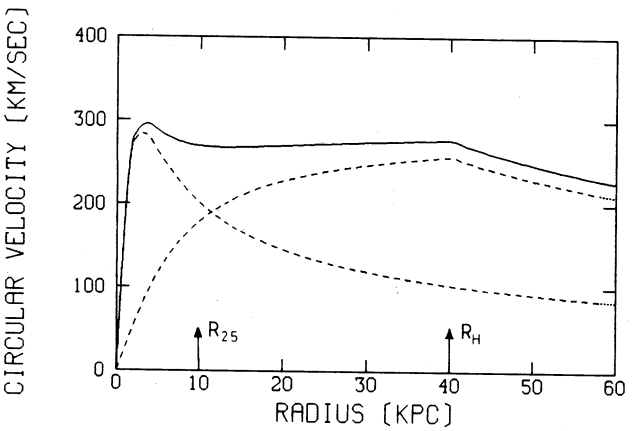

Fig. 1. Rotation curve of model galaxy. The plateau rotational velocity is 290 km s^{-1}, and the ratio $M_{\rm dark}/M_{\rm vis}$ inside R_{25} ($=5\times R_c$) is 0.8. The dashed lines represent the rotation curves for the dark and visible components of the model. The dark halo is truncated at R_H. From this radius outwards, the rotation curve has a Keplerian decline

Figure 2 illustrates two infinitesimal elements of such an integration. The galaxies, HG_1 and HG_2, are separated by r. The element dM_2, in HG_2, on the right, "feels", only partly, the gravitational field of the total HG_1: this is because mass outside r_1, in HG_1, does not exert any force upon dM_2. On the other hand, the element on the left feels the gravitational force of the whole of HG_1. To calculate the force and the potential energy, a double integration has to be performed in the variables r_2 and θ_2, the polar angle (the calculation is axially symmetric about the line joining the two galaxies). The coordinates r_1 and θ_1 are expressed in terms of the integration variables and r (that is kept constant in each integration run).

The only net force component lies in the direction of r. By integration:

$$F(r) = -\int_0^{R_{H2}} \int_0^{\pi} \frac{GM_1(r_1)dM_2(r_2, \theta_2)}{r_1^2} \cos\theta_1, \tag{7}$$

where $M_i = M_{Hi} + M_{Gi}$, $i = 1, 2$, given by Eqs. 2 and 5.

The potential energy, $U(r)$, is obtained from

$$U(r) = \int_0^{R_{H2}} \int_0^{\pi} dM_2(r_2, \theta_2)\Psi_1(r_1), \tag{8}$$

where $\Psi_1 = \Psi_{H1} + \Psi_{G1}$, given by Eqs. 3 and 6.

It is worth mentioning that the overlapping potential of two rigid mass distributions, both represented as superpositions of polytropic distributions, was extensively studied by Alladin (1965) in his investigation of the dynamics of colliding galaxies. The polytropic distributions have integral indices ranging from 0 through 5. Alladin derived numerically the overlapping correction factors over the point-mass potential. The HG model has a mass distribution expressed as the superposition of a polytrope (the Plummer model) and a modified isothermal sphere. Therefore, we cannot use Alladin's results. Moreover, it would be hard to find the right combination of polytropes that, when superposed, could give rise to a rotation curve similar to the one derived using the HG model (Fig. 1), which is very convenient in the present study of binary spiral galaxies.

Figure 3 shows the result of the integration in Eq. 7 (curve HG-HG), and the force profile of an approximate dark halo model, in which the HG mass model is truncated at the binary separation r, and no account is made for the effect of overlapping mass. This means that one galaxy is extended, with radius equal to the binary separation, and the other is a point-mass with the same mass. The galaxies appear less massive as they approach each other.

The two halo-galaxies adopted to produce the curve in Fig. 3 are equal, and have the same parameters as the galaxy represented in Fig. 1.

The behaviour of the approximated dark halo model, when compared to the HG-HG model is not surprising: it overestimates the force, when the overlapping mass in HG-HG is small, and underestimates the force, when the overlapping in HG-HG is large.

3. Orbits in the overlapping potential

We calculate orbits having the apocenter as the starting point. For a given relative velocity at apocenter, we do not know *a priori* what the orbital eccentricity will be. One needs to calculate at least half an orbit, and then with the resulting pericentric separation calculate the eccentricity from

$$e = \frac{r_{apo} - r_{per}}{r_{apo} + r_{per}}. \tag{9}$$

For this reason it is useful to define a parameter that measures the magnitude of the relative velocity at apocenter ($V(r_{apo})$) with respect to the apocentric circular velocity ($V_{circ}(r_{apo})$). We call it α, defined as:

$$\alpha = \frac{V(r_{apo})}{V_{circ}(r_{apo})}. \tag{10}$$

In a Keplerian orbit, α is related to the eccentricity, e, by:

$$e - 1 + \alpha^2 = 0. \tag{11}$$

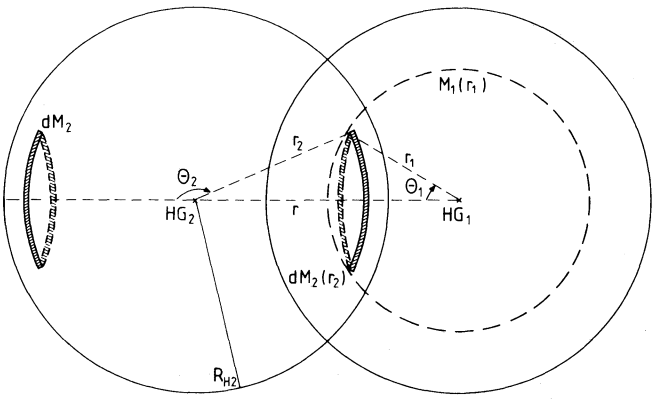

Fig. 2. Two galaxies HG_1 and HG_2, separated by r. For clarity, the visible component is not drawn. The mass element $dM_2(r_2)$, on the right, "feels" only the gravitational attraction from the mass inside r_1, which is equal to $M_1(r_1)$; the mass element on the left feels the entire HG_1. The double integrations shown in Eqs. (7) and (8) are performed in the variables r_2 (from 0 to R_{H2}), and θ_2 (from 0 to π), while r is kept fixed

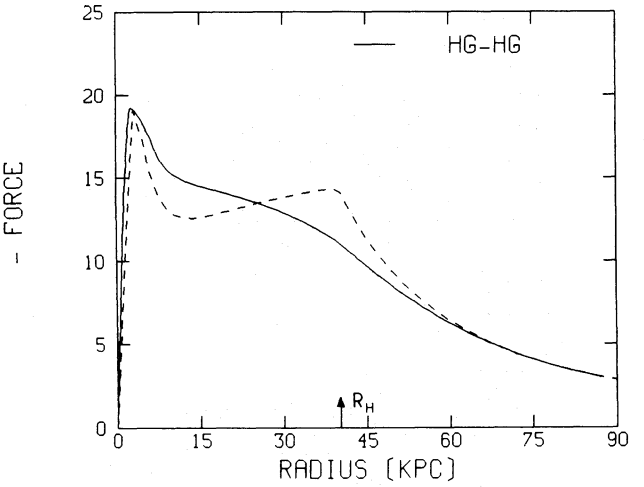

Fig. 3. Radial profile of the binary force field for the truncated dark halo model (HG-HG) as compared to an alternative simplified dark halo model, in which the mass is proportional to the separation, and neglects effects due to overlapping mass distributions

For a pure logarithmic potential a similar relationship between α and c can be derived:

$$\ln\left(\frac{1-e}{1+e}\right)+\frac{2e}{(1-e)^2}\alpha^2=0. \quad (12)$$

The latter case is useful to represent the orbital eccenticity of a point-mass moving in the gravitational field of an extended mass distribution of the type $M(r)\propto r$, a mass law very similar to the HG mass model.

For a given set of model galaxy parameters (M, R_c, σ, a, and R_H) the gravitational force and potential energy, for a binary system, is obtained through a numerical integration of Eqs. 7 and 8. For the orbit calculation we have used the time-centered "*leap-frog*" method. The conservation of energy was better than 0.1%.

The orbits were calculated using two different models, that differ only in the halo size, i.e., in the total mass. For one of the models the truncation radius of the halo is $R_H=4.0$ (total mass of the system is 14.4), and for the other $R_H=8.0$ (total mass is 29.8). For the same initial conditions, the more massive model leads to a less eccentric orbit.

Figure 4 shows three runs characterized by r_{apo} of 4, 8 and 12 units, and $R_H=4.0$. The eccentricities of the model galaxy orbits were, respectively, 0.55, 0.67 and 0.73, for the values of r_{apo} mentioned above. Figure 5 shows orbits for the case $R_H=8.0$, and with the same apocentric separations mentioned above. The orbital eccentricities in this case were 0.51, 0.55, and 0.62. In all cases the Keplerian orbit has the same eccentricity of 0.84.

Note that the orbital properties calculated for these specific models are characteristic for a family of models with the same values for the ratios R_H/R_c and r_{apo}/R_H, and a variable value for the amplitude of the rotation curve.

The basic limitation of our model is that it comprises a rigid mass distribution, that suffers no tidal deformations. Another point refers to dynamical friction, which is nowhere mentioned. These are, however, only apparent limitations. In fact, deformations of any kind, tidal disruption, and dynamical friction are greatly important in a closely interacting system (Barnes, 1988). When such effects begin to operate the binary properties turn out to belong to another group of observables, namely, those which are linked to drastic and destructive events in encounters of galaxies. Moreover, Barnes (1988) has shown that the spherically symmetric N-body galaxies of White (1978, 1979) were very satisfactory in deriving global properties of merging galaxies; many of White's results were confirmed by Barnes' own disk-bulge-halo galaxy encounters. This goes in favour of our spherical model, as far as the antecedent phase of the disruptive event in encounters is concerned, that is precisely the phase we are mainly interested in.

From the consideration of interactive pairs, one can put constraints on the initial properties of a simulated pair, i.e., on its apocentric characteristics (see below). A simulated pair is excluded from the artificial sample, when it has apocentric properties such that in the course of the binary orbit a condition for future merging is eventually achieved. The condition for merging is represented here by an upper limit for the pericentric separation of a pair. What we mean is that for binary approaches closer than this limit separation dynamical friction effects become dominant and lead to a rapid merging process. Therefore, it is useless making a detailed treatment of the binary dynamics in that phase. The potential merger is simply excluded from the simulated

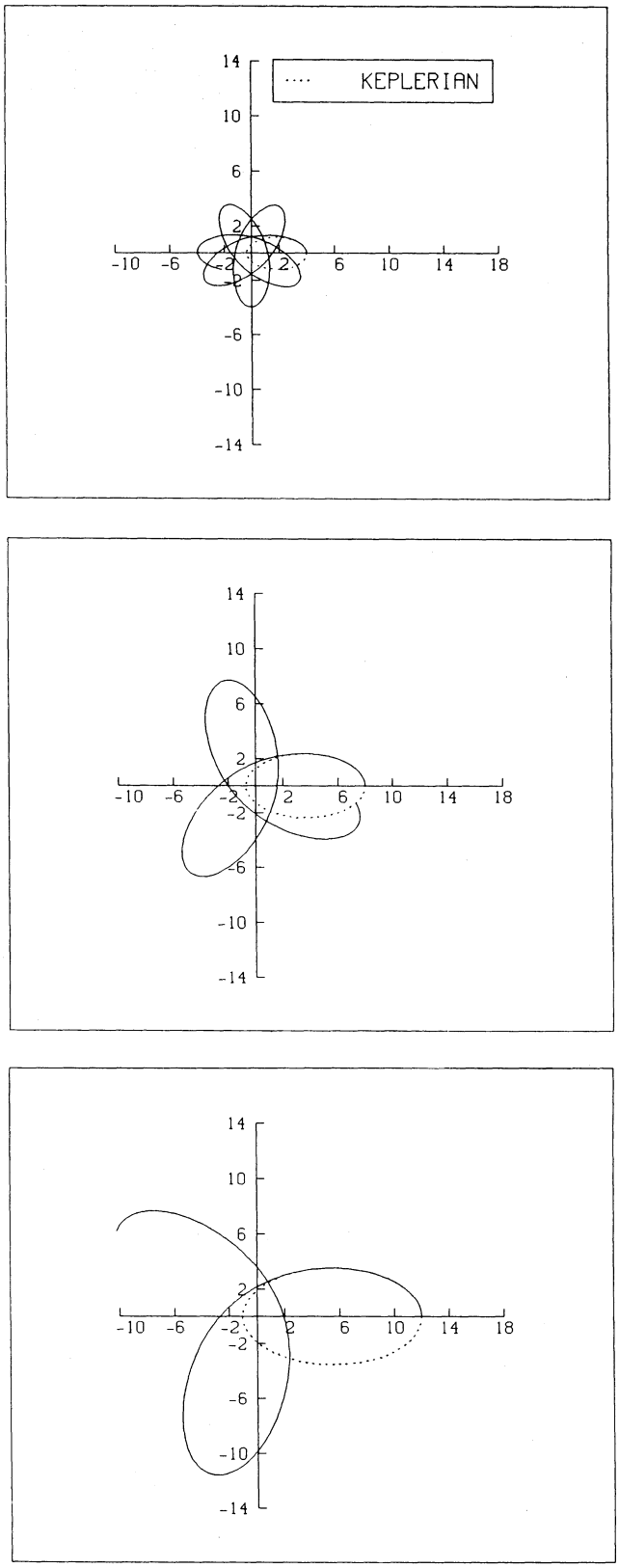

Fig. 4. Orbits of model galaxy binaries, with fixed α, equal to 0.4, and apocentric separations of 4, 8 and 12 units. The dashed ellipses represent the equivalent point-mass orbit, with the same value of α ($e=1-\alpha^2=0.84$). Notice that the halo radius (R_H) is 4 units, and the visible component has a radius of 1 unit

sample. Of course, a reasonable choice for the merging separation must be done. The upper limit for the pericentric separation adopted below, in our simulations, is the value obtained by Schweizer (1987) from a well-defined observed binary sample, which is consistent with the results of simulations of merging galaxies performed by White (1978, 1979) and Barnes (1988). Outside that range of binary separations dynamical friction is neglected, and only the effects of mass overlapping are taken into account.

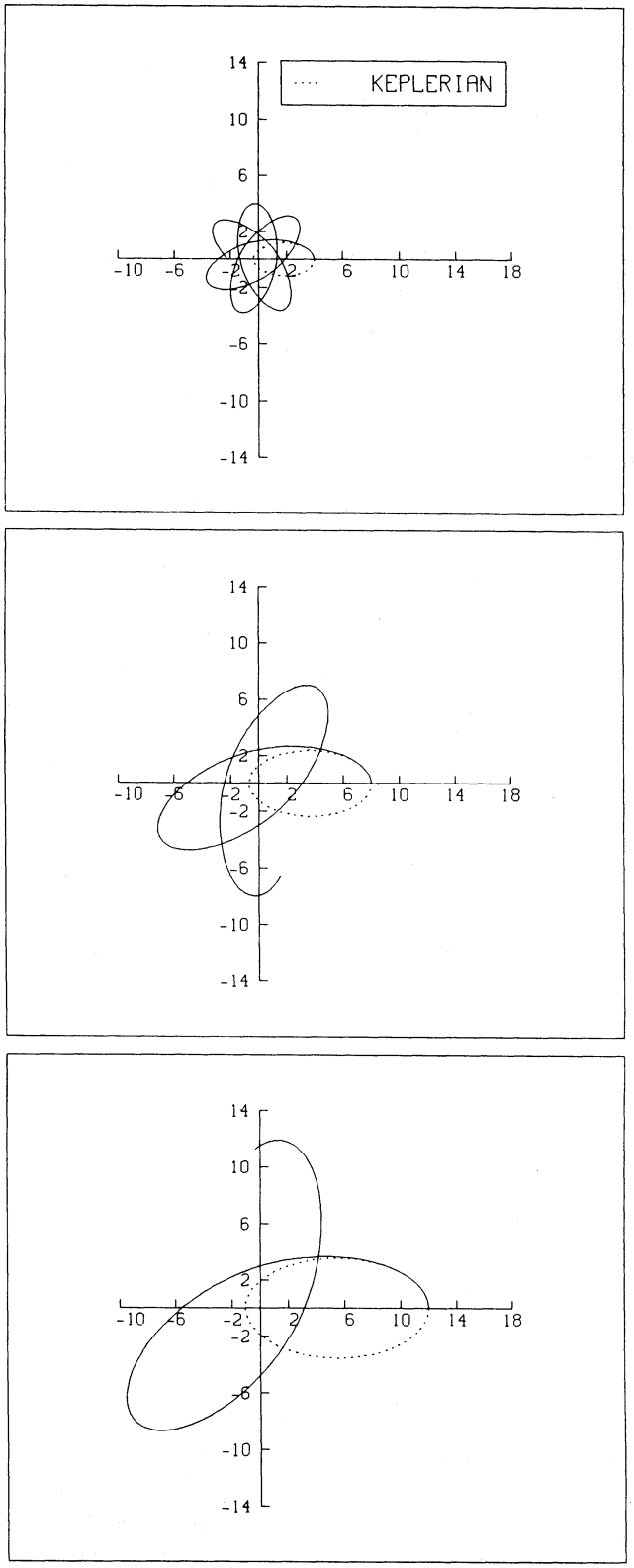

Fig. 5. The same as Fig. 4, for $R_H = 8.0$

4. Monte Carlo simulation of binary galaxies

Monte Carlo simulation of orbits of binary galaxies is a useful tool when we want to analyse an observed binary sample, and this method has been used by many workers in the field (e.g., Turner, 1976; van Moorsel, 1982a; Schweizer, 1987; Oosterloo, 1988). In our case, in which analytical solutions to the binary dynamics cannot be obtained, the Monte Carlo method probably is the best way of analysing binary galaxy data.

We present here the basic notions of our approach and use it to discuss the mass-to-light ratios for the sample of binary galaxies of Schweizer (1987, hereafter LS).

4.1. Description of the simulation procedure

To simulate a sample of binary galaxies, a number of input orbital parameters has to be specified, that is, the distribution of separations, and the distribution of orbital eccentricities. Furthermore, a mass model for the galaxies in a pair has to be defined.

Here, we describe our procedure to simulate a sample of binary galaxies and we apply it to a simple example. The binaries in the example are characterized by fixed apocentric separation, by a given orbital eccentricity distribution, and by two alternative mass models: either a point-mass model, or a halo-galaxy model.

The Monte Carlo algorithm generates 2000 sets of the projected observables, namely, projected relative line-of-sight velocity, and projected separation. All binaries consist of two equal galaxies with a fixed mass. The resulting orbital velocity is later scaled with the square root of the mass. The choice of the input mass for the galaxies is therefore unimportant for the point-mass model, but for the HG model this is no longer true; see below. We adopt as the fixed apocentric separation the value of 200 kpc, which was also used by LS to draw specific conclusions. Our aim is to comment on those conclusions.

In the model fitting algorithm, LS used five trial eccentricity distributions, that sweep the whole range of possibilities from pure circular orbits to nearly pure radial orbits. We concentrate on one of those, the one which was finally regarded as the most suitable to represent real binaries, after the analysis, i.e., $f(e)=2e$ (see LS, Eq. 43(d)). In order to apply it in our simulation, we transform it in a distribution function of the parameter α.

From the fact that $f(e)de = -g(\alpha)\,d\alpha$, we get for the point-mass model:

$$f(e)=2e \Leftrightarrow g(\alpha)=4\alpha(1-\alpha^2). \qquad (13)$$

Here we use Eq. 11, which gives the relationship between e and α.

For the overlapping potential, Eq. 11 is no longer valid. A numerical determination of the corresponding function has to be done in the case of a HG model. In Fig. 6(a), we show these functions for several models, that differ only in the halo size. The dashed curves represent the Keplerian (k) and logarithmic potential (l) cases. We consider in the simulations the same models that were used in the orbital calculations. They have $R_H = 4.0$ ($=40$ kpc), and $R_H = 8.0$ ($=80$ kpc). A third-order polynomial was fitted to the corresponding functions, and the same procedure

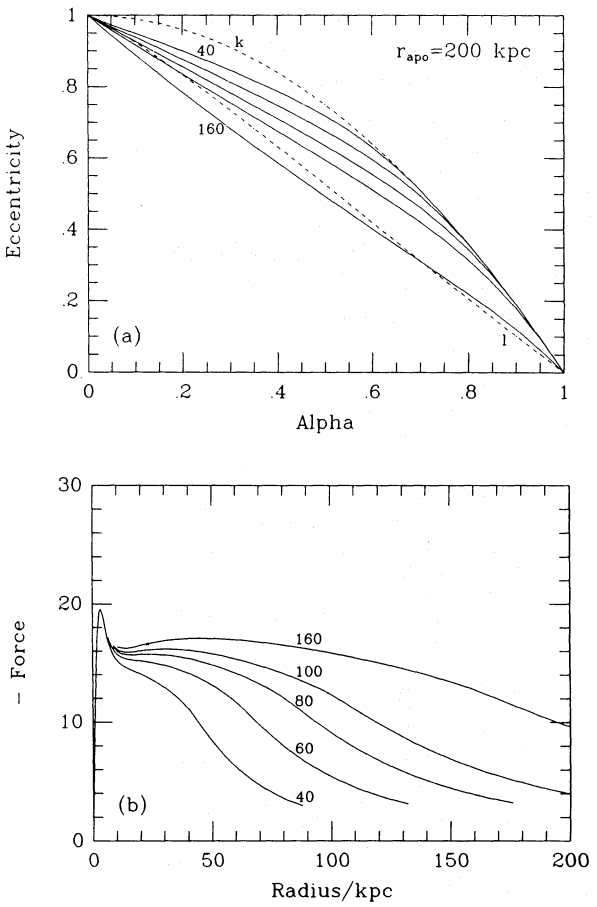

Fig. 6. **a** The functions $e(\alpha)$ are shown, as solid curves, for various halo-galaxy models, which differ only in the halo size. The halo radius ranges from 40 to 160 kpc. All of these functions correspond to a binary apocentric separation of 200 kpc. The dashed curves represent the Keplerian (label k) and logarithmic potential (label l) cases. **b** The force profiles for the same models used in determining the functions $e(\alpha)$. At small separation ($r \leq 20$ kpc) all models give about the same force

applied in deriving Eq. 13 was used. In this way, we get the equivalent α-distributions of the triangular eccentricity distribution, in the case of the HG-models. It is important to notice that, in contrast with the Keplerian and pure logarithmic potential cases, the function $e(\alpha)$ in the overlapping potential case is in reality a function of the form $e = e(\alpha, R_H, r_{apo})$. This means that the curves shown in Fig. 6(a) refer only to $r_{apo} = 200$ kpc. Figure 6(b) shows the radial force profiles of the various binary models used in the orbital calculations to derive the curves in Fig. 6(a).

The series of simulations are done with either the distribution of α given by Eq. 13, in the case of the point-mass model, or with the numerical α-distributions, determined as described above, in the case of the HG-models. All of these distributions are equivalent to a triangular distribution in e, favouring "*moderately high eccentricity orbits*", as stressed by LS.

When investigating the possibility of merging in the observed sample, LS put forward two conditions that should be obeyed by potential mergers. These conditions were

$r_{min} \leq 0.7\rho$

and

$$\textit{Orbital period} \leq \frac{1}{2}\,\textit{Hubble time.}$$

Here r_{min} is the value of the pericentric separation and ρ is the median value of the sum of the radii of the galaxies for a pair, as derived from LS's observed sample (which gave $\rho = 38$ kpc). LS used these criteria to estimate the effect of mergers, as part of an attempt to understand the selection biasses operating on the observed distribution of separations. The constraints imposed by mergers on the properties of the simulated pairs were, however, not explicitly taken into account by LS. Now, for the above mentioned apocentric separation the orbital period is always smaller than 1/2 *Hubble time*. This means that all pairs with orbits with $r_{per} \leq 27$ kpc will have merged.

The simulation of one binary is done with the following steps: (*a*) a value of α is obtained from the proper distribution, according to the mass model being used; (*b*) $V(r_{apo}) = \alpha \times V_{circ}(r_{apo})$ is calculated; (*c*) if we want to restrict the separation of the galaxies in the binary system, the "*merging test*" is done using the conservation laws of energy and angular momentum. This test verifies if the pair will have a pericentric separation (r_{per}) smaller than 27 kpc. If this is true, the algorithm begins again at (*a*). Otherwise, it goes to the next step. If no restriction is to be considered, the test is not done, and the next step follows; (*d*) A half-orbit is calculated, i.e., the binary path from apocenter to pericenter. Due to the characteristics of the force field, this orbit segment is fully representative of the time evolution of the system; (*e*) the half-orbit is rotated by a random angle, in the orbital plane. This simple procedure mimics the evolution of the binary over a long time scale. (*f*) An orbital inclination i is obtained according to $F(i) \propto \sin i$, i.e., the normal to the orbital plane is distributed at random in space. (*g*) Projected separation in the plane of sky, and line-of-sight velocity difference are calculated, at a random time instant within the orbit half-period, as well as other relevant quantities, such as orbital eccentricity, orbital period, etc.

This sequence is the same regardless of the mass model adopted. Of course, for the point-mass model it would not be necessary to perform a numerical orbital calculation because the analytic solution for the problem is known. For the sake of uniformity, we adopt, for both the point-mass and the HG model, a numerical approach.

The Monte Carlo simulations done here, for the sake of illustration of our method, incorporate a feature that, although simple by itself, is of fundamental importance, and has been absent in many of relevant previous studies of binary galaxies. We talk about step (*c*), in the basic recipe for performing the generation of an artificial pair.

That step, called the "*merging test*", is a procedure which mimics the effect of merging, and excludes from the simulated sample all possible mergers. Though, here, it is still a very soft criterium against mergers (see White, 1978, 1979, and, Aarseth and Fall 1980, where hard criteria are derived from N-body simulations of merging galaxies), such preoccupation is completely disregarded in the simulations done by Turner (1976) and Schweizer (1987). As far as we can judge, this very decisive point was by its first time adopted by van Moorsel (1982a, 1987) in his careful and detailed study of a binary sample; the same procedure was later used also by Oosterloo (1988) in his study of angular momentum in binary galaxies.

In fact, the softness of our merging test is only true, if galaxies have an extended dark component. We state the condition for merging as a rejection of any trial, if the binary spatial separation would get smaller than approximately the sum of the visible radii of binary members, at some position in the orbit.

4.2. *Simulations*

Figure 7 presents the results of the simulations described above. They are displayed in the same frame of coordinates used by LS, with the only difference that we adopt here another system of units: the projected separations are given in units of 10 kpc, and the normalized projected velocity difference in units of 3.09×10^{-4} km s$^{-1} \times M_{\odot}^{-1/2}$. For a $1 \times 10^{11}\ M_{\odot}$ binary system, this means that one unit of projected velocity difference corresponds to 97.8 km s^{-1}.

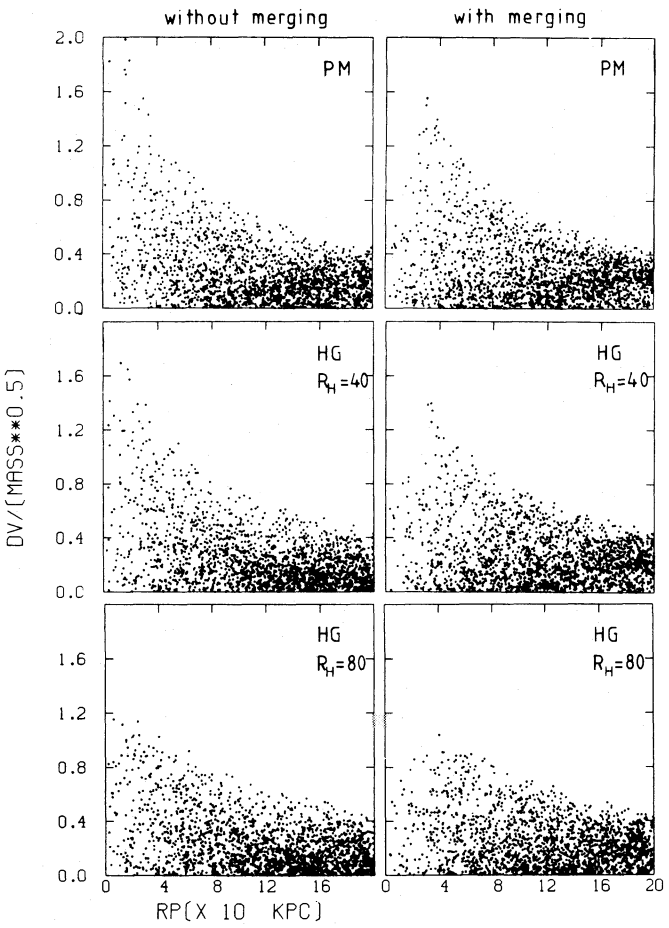

Fig. 7. Monte Carlo simulations of binary galaxies with fixed apocentric separation $r_{apo} = 200$ kpc. In the top panels galaxies are point masses, middle panels represent halo-galaxy binaries, with halos truncated at $R_H = 40$ kpc (4.0 units), and the bottom ones are HG-binaries, with $R_H = 80$ kpc (8.0 units). The left panels represent binaries that were not restricted by the merging test. The right panels show binaries which have suffered the merging test, and can not approach more than 27 kpc (LS's "merging" radius). It is clear that strict point-mass galaxies can have very high velocity differences at small separations. This does not happen with the other cases: even the HG-binary model with the smaller halo, not subjected to the merging test, shows a deficiency in that region of the diagram. The unit of the vertical axis is 3.09×10^{-4} km s$^{-1} \times M_{\odot}^{-1/2}$. The top left diagram can be directly compared with diagram (d) in Fig. 17 of LS

The top panels refer to point-mass binaries, the middle panels to HG-binaries, with $R_H = 4.0$ units, and the bottom ones to HG-binaries, with $R_H = 8.0$ units. To the binaries in each of the three left panels the "merging" restriction was not applied, and those on the right panels were affected by the merging test described above. The top left panel is analogous to the simulation shown in LS's Fig. 17(d).

The main effect of the use of orbits for extended masses on the distribution of the points in the velocity-separation diagram in Fig. 7 is the depopulation of the region of large velocity differences at small projected separations. The introduction of merging criteria depopulates this region even further. The effect of the latter would be more pronounced in the case of smaller apocentric separations, because in that case more high eccentric orbits would be forbidden. In Fig. 7 the merging criteria introduce a cut-off in the eccentricity distribution, at a value of $e_{max} = 0.76$, in all simulations with "mergers". This value corresponds to orbits that have the minimum allowed pericentric separation, i.e., 27 kpc.

When we increase the galaxy mass, both point-mass diagrams do not change at all (the vertical axis has velocity differences normalized by the square root of the total binary mass). This is not quite true, however, with the HG-models. Increasing the mass, here, by increasing the halo size modifies the force profiles (see Fig. 6(b)). As we can see, in Fig. 7, the two different HG-model binaries, with different total masses, have small but noticeable differences in the distribution of points in the diagrams. The more massive binaries have comparatively smaller maximum velocity differences.

In conclusion: the largest discrepancies between the various simulations in Fig. 7 show up in the small separation range. It is in this range that both the merging criteria and the overlapping corrections for the potential are important. When one looks to the large separation range all simulations are remarkably similar. Because of this, *the high velocity difference values at small projected separations in an observed sample should be considered with care.*

5. Discussion: mass-to-light ratio in Schweizer's sample

LS concluded that binary galaxies can be represented fairly well by point masses moving in somewhat high eccentric orbits, that is, with a frequency distribution function of eccentricities given by $f(e) \propto e$. One of the clues for this conclusion was the fact that LS obtained high velocity differences, at small separations, in simulations that were characterized by a distribution of that kind, a feature that is also present in the observed sample. Figure 8 shows the observed data used by LS. The observed velocity differences are normalized to equal-luminosity binaries ($L_{tot} = 10^{11}\ L_{V\odot}$, $H_0 = 50$ km s^{-1}/Mpc), and are given in the units used here, i.e., 97.8 km s^{-1}. The results presented in Sect. 4 show that, in addition to the orbital eccentricity, the shape of the mass distribution in the galaxies and merging have a pronounced effect on the population of the high velocity difference-small projected separation region.

LS argues also that the great concentration of points in the region of both small velocity difference and small projected separation could be accounted for by binary orbits of high eccentricity, and with small apocentric separation. Of course that would be an easy way of populating that area, if merging

processes are not effective. We suggest, in the light of the simulations presented above, that this is not the case, and, as a consequence, the only way of getting those points is with binaries in orbits that have low eccentricities and relatively small apocentric separations. It is obvious that circling speeds at small binary separations are large, but projection effects make it possible to populate the whole range of velocities below the relative velocity at r_{apo}, and of separations below r_{apo}. For an illustration, see, for example, LS's Fig. 17(a), that shows a simulation of pure circular orbit binaries with fixed apocentric distance.

One cannot draw any firm conclusion from a comparison between the simulations shown in Fig. 7, and the observed data. The observations are contaminated by a number of selection effects, and by the presence of unbound ("optical") pairs, that must be taken into account in the comparison. Moreover, the simulations refer to binaries with fixed apocentric distance, which is certainly not true for the binaries in the observed sample. A qualitative result can be obtained, though, by trying to match a given observed binary shown in Fig. 8 with the simulated points. For the sake of illustration, one can take the observed binary with velocity difference equal to about 5.4 units and projected separation of 20 kpc (see point indicated by arrow in Fig. 8), and require that it lies close to the upper envelope of the points in the various panels of Fig. 7. (This is LS's pair no. 4, which was assigned a probability of 0.88 of being bound). By equating the observed value of $\Delta V/\sqrt{L}$ to the value of $\Delta V/\sqrt{M}$ in the models, a value of M/L is obtained. The models without merging fit the observation with M/L values of approximately 7, 11, and 22, the lowest value being found for the point-mass model. The respective values for the models with merging are considerably larger, namely, 22, 34, and 39.

The evidence obtained here indicates that the combined effect of extended masses and merging processes can introduce fundamental changes in LS's result, probably giving a quite different conclusion with respect to the orbital characteristics of the binaries. This fact would at the same time modify sensibly the derived mass-to-light ratio.

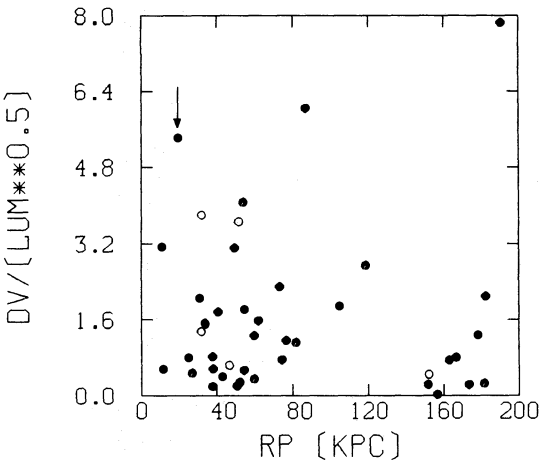

Fig. 8. Schweizer's (1987) observed sample of 48 binary galaxies. The filled circles represent pairs in which at least one of the galaxies is a spiral (there are 31 pairs with only spirals, and 11 with just one spiral galaxy). Then open circles represent pairs that have no spiral galaxies. The vertical axis has velocity differences normalized to an equal total luminosity of $10^{11}\,L_{V\odot}$. The unit is $3.09\times10^{-4}\,\mathrm{km\,s^{-1}}\times L_{V\odot}^{-1/2}$. A similar diagram is shown in LS's Fig. 5, where the velocity difference values must be divided by $97.8\,\mathrm{km\,s^{-1}}$ to be consistent with the units we use here. The fiducial point adopted in the discussion is indicated by an arrow

6. Conclusion

The model adopted for the dark halo has been extensively and successfully used by Kent (1987) in his modelling of the dark matter distribution in spiral galaxies. A modified version of the same model has been also adopted in other investigations (e.g., Begeman, 1987; van Albada and Sancisi, 1986; van Albada et al., 1985; Bahcall and Casertano, 1985). The unique characteristic of our approach is the truncation of the halo outer radius. The idea, of course, is to determine the radius of the dark halo through the analysis of a binary galaxy sample. If the halo radius is small (20–30 kpc in radius) the result is consistent with the point-mass approximation. On the other hand, if real galaxies have extended and large dark halos (as implied by observed "flat" rotation curves of spiral galaxies), our study predicts unambiguous features in the distribution of binary galaxy properties. It is not surprising that the difference between the small-halo HG model and the PM model is not large. Particularly, the PM model, with merging, is indistinguishable from the HG model with halo radius equal to the merging radius (27 kpc, see Sect. 4.1). In turn, it is interesting to notice the clearly detectable differences between the PM (or small-halo HG) model and the large-halo HG model. The main conclusion is that the HG model can introduce fundamental changes in LS's result, if spiral galaxies have extended and large dark halos as inferred from observed rotation curves.

A more conclusive answer to questions posed by double galaxy systems is most likely to be obtained with the more complete mass model for binary galaxies presented here. Finding the best model which fits to an observed sample means untangling the effects of orbital eccentricity and halo size (i.e., galaxy total mass). This was already recognized by Turner (1976). If this achievement was difficult in earlier investigations, it proves possible now, with a better model for binary galaxies, and an improved binary catalogue, with highly accurate data (see T. S. van Albada and D. S. L. Soares, *in* Soares, 1989).

A detailed statistical study, taking care of selection effects in the determination of the binary catalogue in use, will lead to answers to important questions: what is the size of galactic dark halos?, and, what is the orbital eccentricity distribution in binary galaxies? An investigation of the first of these questions has been done in Soares (1989).

Acknowledgements. It is a great pleasure to thank T.S. van Albada and R.H. Sanders for many useful discussions and suggestions during all stages of this work, and specially for having suggested me this investigation. The initial manuscript was considerably improved due to their comments. I also thank T.R. Bontekoe who was very kind in helping me in the calculation of the overlapping potential, and T.A. Oosterloo for very useful and enlightening discussions in the 'early stages of this work. Finally, I would like to thank the partial support by the Brazilian Agency CAPES, Coordenação de Aperfeiçoamento de Pessoal de Nível Superior (Proc. No. 7382/84-12).

References

Aarseth, S.J., Fall, S.M.: 1980, *Astrophys. J.* **236**, 43

Albada, T.S. van, Bahcall, J.N., Begeman, K., Sancisi, R.: 1985, *Astrophys. J.* **295**, 305

Albada, T.S. van, Sancisi, R.: 1986, *Phil. Trans. Roy. Soc. Lond. A* **320**, 447

Alladin, S.M.: 1965, *Astrophys. J.* **141**, 768

Bahcall, J.N., Casertano, S.: 1985, *Astrophys. J.* **293**, L7

Barnes, J.E.: 1988, *Astrophys. J.* **331**, 699

Begeman, K.G.: 1987, Ph.D. Thesis, University of Groningen

Borne, K.D.: 1988, *Astrophys. J.* **330**, 38

Holmberg, E.: 1937, *Lund. Ann.* **6**, 1

Karachentsev, I.D.: 1985, *Soviet Astron.* **29**, 243

Kent, S.M.: 1987, *Astron. J.* **93**, 816

Moorsel, G.A. van: 1982a, Ph.D. Thesis, University of Groningen

Moorsel, G.A. van: 1982b, *Astron. Astrophys.* **107**, 66

Moorsel, G.A. van: 1987, *Astron. Astrophys.* **176**, 13

Oosterloo, T.A.: 1988, Ph.D. Thesis, University of Groningen

Page, T.: 1952, *Astrophys. J.* **116**, 63

Peterson, S.: 1979, *Astrophys. J.* **232**, 20

Rubin, V.C., Burstein, D., Ford, W.K., Jr., Thonnard, N.: 1985, *Astrophys. J.* **289**, 81

Schweizer, L.Y.: 1987, *Astrophys. J. Suppl. Series* **64**, 427 (LS)

Soares, D.S.L.: 1989, Ph.D. Thesis, University of Groningen

Turner, E.L.: 1976, *Astrophys. J.* **208**, 304

White, S.D.M.: 1978, *Monthly Notices Roy. Astron. Soc.* **184**, 185

White, S.D.M.: 1979, *Monthly Notices Roy. Astron. Soc.* **189**, 831

White, S.D.M.: 1981, *Monthly Notices Roy. Astron. Soc.* **195**, 1037

White, S.D.M., Huchra, J., Latham, D., Davis, M.: 1983, *Monthly Notices Roy. Astron. Soc.* **203**, 701